J Mater Sci (2013) 48:8215–8227
DOI 10.1007/s10853-013-7633-x

Anti-microbial and anti-corrosive poly (ester amide urethane) siloxane modified ZnO hybrid coatings from *Thevetia peruviana* seed oil

T. O. Siyanbola · K. Sasidhar · B. Anjaneyulu · K. P. Kumar · B. V. S. K. Rao · Ramanuj Narayan · O. Olaofe · E. T. Akintayo · K. V. S. N. Raju

Received: 12 June 2013 / Accepted: 25 July 2013 / Published online: 10 August 2013

Abstract The utilization of renewable resources for the development of organic coatings is a viable means of creating alternatives to petroleum-based chemicals which are not eco-friendly. This paper reports the synthesis of polyesteramide–urethane–silica–zinc oxide hybrid coatings from *Thevetia peruviana* seed oil (TPSO). The periphery of ZnO nano-particles is modified with 3-aminopropyltrimethoxysilane to prepare silica grafted ZnO composite particles. The TPSO based polyesteramide was reacted with 4,4′-diisocyanatodicyclohexylmethane in presence of siloxane modified ZnO to obtain –NCO terminated polyesteramide–urethane–silica ZnO prepolymer. These hybrid pre-polymers were casted on tin foil and cured under atmospheric moisture to obtain eco-friendly, moisture cured polyesteramide–urethanes–silica–zinc oxide hybrid coating films. The synthesized polyester and polyurethane formation was confirmed by using FT-IR and NMR spectroscopic techniques. The resultant hybrid coating films were characterized by using FT-IR, TGA, DSC, SEM, corrosion resistance and microbial resistance. Results confirm that with increase of siloxane modified ZnO content in the polyurethane matrix thermal stability, glass transition temperature and corrosion resistance improved. The antibacterial activity shows that the hybrid films exhibit excellent resistance towards *Escherichia coli* and *Staphylococcus aureus*. The salt spray test on coated panel samples show good corrosion resistance properties.

T. O. Siyanbola
Chemistry Department, College of Science and Technology, Covenant University, P.M.B. 1023, Ota, Ogun State, Nigeria

K. Sasidhar · R. Narayan · K. V. S. N. Raju (✉)
Polymers and Functional Materials Division, Indian Institute of Chemical Technology, Hyderabad 500007, India
e-mail: kvsnraju@iict.res.in; drkvsnraju@gmail.com

B. Anjaneyulu
Centre for Lipid Research, Indian Institute of Chemical Technology, Hyderabad 500007, India

K. P. Kumar · B. V. S. K. Rao
Biology Division, Indian Institute of Chemical Technology, Hyderabad 500007, India

O. Olaofe · E. T. Akintayo
Chemistry Department, University of Ado-Ekiti, P.M.B. 5363, Ado-Ekiti, Nigeria

Introduction

Over the years, organic coatings have been formulated based on petroleum products for corrosion protection. The depletion of this natural resource and the global crisis centred around it, coupled with various environmental issues such as petroleum gas flaring, oil spillage and other generated industrial and domestic wastes that are discharged into the environment [1–4], makes it imperative that petroleum feedstock be substituted with sustainable resource materials, such as vegetable oils, natural rubber, proteins, cellulose and starch, which are capable of providing chemicals and polymeric materials that will match or surpass the qualities provided by petroleum products [5–7].

Organic coatings such as polyurethanes, epoxies, alkyds, polyesteramide, polyetheramides and other polymeric resins [8–11] have been prepared from different vegetable oils like castor, linseed, pongamia, nahar, soya bean, tung oil, annona squamosa and others [12–18]. These resins are well known in the industrial sector towards the production of varnishes [19], surface coatings [20], plasticizers, thermal stabilizers [21], lubricants [13] and anticorrosive materials [10, 22]. The types of industrial products obtained from

these vegetable oils depend on their fatty acid profile of the oils. These fatty acids usually make up to 94–96 wt% of the triglyceride [7, 23]. The types of industrial products obtained also depend on the way the oils are modified [24] e.g. epoxidation, hydrolysis, urethanation, boiled oil, metathesis, aminolysis, and halogenation [13]. Aminolysis is a useful modification route on triglycerides that leads to the formation of a monomer known as *N*,*N*′-bis(2-hydroxyethyl) fatty amide [13, 25]. The hydroxyl functionality on this monomer provides the active site for preparing the polyesteramide and for the subsequent urethanation. Polyurethanes are well known for their good adhesion, high toughness, good water and acid resistance, as well as excellent abrasion resistance [10, 26]. These are the reasons why polyurethane polymers especially those synthesized from diol-based polyesteramides, are widely used in organic coatings [10, 27, 28]. However, the reinforcement of the polyesteramide–urethane polymer matrix with fillers, such as nano materials, is said to give better toughness, strength, thermal stability and reduction of curing time, chemical and environmental resistance which invariably will improve the performance of the polymer composites [29]. Polymeric composites have found uses in the following industries: oil and gas, marine, aviation, automobile, military and civil construction; they are also useful in packaging materials, contact lenses, and other applications [7, 30]. Among all the nano materials, Zinc-based materials are proven to be an excellent resistance against corrosion and exhibit good antibacterial and anti-fungal activity [29–35]. Mishra et al. [36] incorporated ZnO nano-powder within a polyurethane matrix and their study reveals that as the percentage of the nano-material increases in the formulation, the adhesive strength also increases. This effect is due to the ZnO surface geometry which constrains the –NH groups of the urethanes/urea moieties from making hydrogen bonds with the C-O groups in the hard segment. However, there is difficulty in the dispersion of the nano-materials within the polymer matrix as the percentage quantity increases hence, there is a necessity of modification of the hydroxyl peripheral of nano ZnO [44]. The peripheral modification of ZnO with 3-aminopropyl-triethoxysilane and its infusion in the polymer matrix of hyper-branched polyurethane was carried out by Jena et al. [37] of which the thermal degradation, corrosion, and impact resistance of the prepared composites were studied. In this study, we set about the modification of the ZnO periphery with 3-aminopropyl-trimethoxysilane (APTMS) which was coupled with polyurethane material prepared from a bio-based renewable source (*Thevetia peruviana* seed oil [TPSO]).

Literature survey on TPSO reveals that it has never been used as a base material in the synthesis of organic coatings. However, reports on the physico-chemical properties of the seed oil with respect to location of harvest [38] as well as the insecticidal, rodenticides mollusicidal and antibacterial examinations on the seed oil and leaves of the plant have been reported [39, 40]. *T. peruviana* is an ornamental evergreen shrub and commonly known as Lucky Nut, Digoxin, Yellow Oleanda belongs to the Apocyanaceae family [38, 41]. The sub-tropical plant is native to Central and South America [38].

The present work attempts to synthesis *N*,*N*′-bis (2-hydroxy ethyl) *T. peruviana* fatty amide (HETA) from TPSO and through the condensation polymerization of HETA and isophthalic acid, polyesteramide of *T. peruviana* (TPPEA) was also synthesized. Hybrid-NCO terminated poly (urethane *Thevetia* fatty amide) resin (PUTFA-APTMS-ZnO) was synthesized by the reaction of 4,4′ diisocyanatodicyclohexylmethane (H_{12}MDI) and the polyesteramide diol TPPEA with varying percentages of siloxane modified ZnO.

Experimental

Materials

Thevetia peruviana seeds were collected from the compound of Alhaji and Alhaja R.A. Amodu at Emure-Ekiti, south-western Nigeria. The air-dried seeds were grounded to a powdered form and oil extraction was carried out using the Soxhlet apparatus with *n*-hexane as solvent. The fatty acid composition of the oil was carried out using a gas chromatography (GC; HP-1 ms, 30 m × 0.25 mm × 0.25 μm, FID detector). The diethanolamine, *n*-hexane, diethyl ether, isophthalic acid, xylene, 4-methyl pentan-2-one, anhydrous sodium sulphate was obtained from S.D. Fine Chemicals (Mumbai, India). AR sodium methoxide from Avra chemicals (Hyderabad, India) and 4,4′-diisocyanatodicyclohexylmethane (H_{12} MDI) from Alfa Aesar chemical UK were procured. ZnO nano powder (particle size 50–70 nm) was purchased from Aldrich (Milwaukee, WI).

Methods

The FT-IR, ^{1}H NMR was used to characterize the chemical structure of HETA, TPPEA, PUTFA, PUTFA-ZnO (5 wt%), PUTFA-APTMS-ZnO (5 wt%), PUTFA-APTMS-ZnO (10 wt%), and PUTFA-APTMS-ZnO(15 wt%). FT-IR spectra of the resin were taken over KBr on Perkin Elmer spectrum 100 spectrometer (PerkinElmer Inc. USA) by scanning eight times. ^{1}H NMR and ^{13}C NMR were respectively recorded on Varian VXR-Unity 200 MHZ spectrometer and Bruker UXNMR 400 MHZ spectrometer by using $CDCl_3$ and DMSO-d_6 as a solvent and teramethyl

silane as an internal standard. The thermal stability of the hybrid resins and curing behaviour were studied by thermogravimetric analysis (Perkin Elmer TGA 7, TA Instrument, and USA) and differential scanning calorimetry (Perkin Elmer TA DSC Q100 USA) at a constant heating rate of 10 °C min^{-1} in nitrogen atmosphere. The morphology study was carried out on SEM Hitachi-S520 (Oxford link ISIS-SEM model), Japan. Elcometer was used in taking the thickness of the coatings on metal steel panels. Refractometer RFM 800 instrument was used to calculate Refractive index of all resin samples.

In vitro antimicrobial activity of the polymers was studied and tested against Gram-positive organisms viz. *Bacillus subtilis* (MTCC 441), *Staphylococcus aureus* (MTCC 96) and Gram-negative organisms viz. *Escherichia coli* (MTCC 443), and *Klebsiella pneumoniae* (MTCC 618) by agar diffusion method [42]. The ready-made nutrient agar was suspended in distilled water (1000 mL) and heated to boiling until it dissolved completely; the medium and petri dishes were autoclaved at pressure of 15 lb inc^{-2} for 20 min. The medium was poured into sterile petri dishes under aseptic conditions in a laminar air flow chamber. When the medium in the plates solidified, 0.5 mL (approx. 10^6 CFU ml^{-1}) of culture of test organism was inoculated and uniformly spread over the agar surface with a sterile L-shaped rod. embedded polymer samples with 2 × 2 cm (approx) samples were washed with double distilled water and placed on the medium and incubated at 37 °C (bacteria) for 24. Uncoated polymers were used as controls. The antibacterial activity was performed based on the formation of inhibition zone loss of growth of organism beneath and surroundings of the films placed on agar medium. Three replicates were maintained for each treatment. MTCC is the microbial type culture collection in IMTECH (CSIR LAB) Chandigarh, India.

Silicon carbide papers of varying grades were used for the preparation of mild steel strips; which were washed with water, ethanol and acetone. The degreased metal strips were dried under vacuum for hours. The pristine and hybrid coatings were prepared by brush application of 60 wt% of resin in xylene on the mild strips. For chemical resistance test in water, acid (5 wt% HCl), alkali (5 wt% NaOH) taking in 3 inches diameter porcelain dishes standard sizes of mild strips of 30 × 10 × 1 mm^3 were used. The salt spray tests were carried out in a salt mist chamber following ASTM B 177-94 standard. A 3.5 wt% NaCl solution was atomized by compressed air in the chamber containing the specimen.

Synthesis of *N*,*N*′-bis (2-hydroxyethyl) *T. peruviana* oil fatty amide (HETA)

The preparation of HETA was carried out in a four neck round bottom Pyrex flask containing diethanolamine and TPSO fitted with mechanical stirrer, condenser, and thermometer, the flask was submerged in an oil bath. With a molar ratio of 6:1 diethanolamine and oil in the presence of 2 % sodium methoxide was reacted at 115 °C. The progress of the reaction was monitored by TLC. At the completion of the reaction, the reaction mixture was allowed to cool and it was dissolved in diethyl ether in a separating funnel. The ethereal layer was washed with 5 % aqueous hydrochloric acid. The ether layer was separated and washed with water and later dried over anhydrous sodium sulphate. Rotary evaporator was used in concentrating the ether layer [43].

Synthesis of *T. peruviana* polyesteramide (TPPEA)

TPPEA was synthesized by reacting HETA (0.0584 mol) with isophthalic acid (0.0292 mol) and 27 ml xylene as solvent in a four neck round bottom flask connected to a Dean stark, thermometer, mechanical stirrer, and a nitrogen inlet tube. The reaction mixture was refluxed at 145–150 °C until the theoretical amount of water was collected and the reaction was monitor by the determination of acid value at regular intervals [44]. At the end of the reaction the product (TPPEA) was taken out of the four neck round bottom flask and xylene (solvent) was withdrew from the compound using rotary evaporator under reduced pressure.

Preparation of APTMS modified ZnO

In a 500 ml round bottom flask, 50 g toluene and 10 g ZnO powder were added and stirred for 10 min using a magnetic stirrer 30 min of ultrasonic bath was carried out so as to make uniform suspension. To this suspension, 1 g of APTMS was added and the resulting mixture was stirred at room temperature for 1 h. A slightly yellow-transparent coloration was obtained. The reaction mixture was refluxed for 24 h. Rotary evaporator was used to removed the solvent form the APTMS modified ZnO (APTMS-ZnO). Unreacted APTMS was removed by washing the compound with ethanol. The powder was dried at 50 °C for 1 h in an oven. The modified powder was grinded and further dried at 100 °C for 2 h [37].

Synthesis of hybrid-NCO terminated poly (urethane fatty amide) resin (PUTFA-APTMS-ZnO)

TPPEA (5.08 g) was dissolved in 4-methyl pentan-2-one and calculated amount of APTMS-ZnO was added (5, 10, 15 wt%) and kept it on ultrasonic bath. To a three neck round bottom flask fitted with nitrogen gas inlet, thermometer, and dropping funnel, 1.34 ml H_{12}MDI was added to a 1 ml 4-methyl pentan-2-one under stirring. The

TPPEA and ZnO-APTMS mixture was slowly added into the round bottom flask, the reaction mixture was then heated at 75 °C for 3 h. The progress of the reaction was monitored by TLC and hydroxyl value determination. Pure PUTFA as well as PUTFA-ZnO (5 wt%) (i.e. unmodified ZnO) coating films were also prepared. Finally, the pristine and hybrid nano-composites films were obtained by casting the solution on a tin foil and mild steel panels and allowed to cure at ambient temperature. After curing tin foil was removed by amalgamation with mercury to get free films. Cured films (with 5 μm and 100–120 μm thickness for foil and mild steel panels respectively) were coded as PUTFA, PUTFA-ZnO (5 wt%), PUTFA-APTMS-ZnO (5 wt%), PUTFA-APTMS-ZnO (10 wt%), and PUTFA-APTMS-ZnO(15 wt%) where 5, 10, and 15 corresponds to wt% of nanoparticles in the polymer matrix.

Results and discussions

The reaction schemes for the synthesis of HETA, TPPEA, PUTFA, and its hybrid modified forms (PUTFA-ZnO [5 wt%], PUTFA-APTMS-ZnO [5 wt%], PUTFA-APTMS-ZnO [10 wt%], and PUTFA-APTMS-ZnO [15 wt%]) are presented in Schemes 1, 2, 3 and 4 below. TPSO in the presence of sodium methoxide as catalyst reacts with diethanolamine to form HETA (Scheme 1). Synthesis of TPPEA by the combination of HETA and isophthalic acid may result in the formation of polyesteramide (Scheme 2). Preparation of modified ZnO particle with APTMS (Scheme 3). Finally, the addition of reaction products mixture of Scheme 2 and 3 with H_{12}MDI in the presence of varying percentages of the nanocomposite to form PUTFA and its hybrid forms (Scheme 4).

FT-IR and NMR spectral analysis

N,N′-bis (2-hydroxyethyl) T. peruviana oil fatty amide (HETA)

Figure 1 shows the overlay FTIR spectra of HETA and that of TPPEA. HETA has a characteristic broad –OH adsorption band at 3370.07 cm^{-1}. The CH_2 stretching band for asymmetric and symmetric is observed at 2924.31 and 2853.58 cm^{-1} respectively. The strong C=O stretching vibration of the amide appears at 1622.56 cm^{-1}. The C–N stretching vibration peak is observed at 1466.70 cm^{-1} while 1365.64 cm^{-1} represents C–H bending and 721.94 cm^{-1} represent the bands due to alkene C–H bending mode.

The ^{1}H NMR spectrum for HETA is represented on Fig. 2, the terminal methyl protons of the fatty acid chain is seen at $\delta = 0.89$ ppm, CH_2 within the fatty acid chain is observed at $\delta = 1.25$ ppm. At $\delta = 1.56$ ppm CH_2 two steps from the C=O attached to nitrogen is observed (–**CH$_2$**–CH_2–C=O), CH_2 adjacent to the double bond carbon atom (olefinic carbon) is at $\delta = 2.15$ ppm. CH_2 attached to the C=O group appears at 2.35 ppm, the chemical shift at 3.45 ppm and 3.68 are the methylene group attached to nitrogen and hydroxyl group respectively, the proton on the hydroxyl functional group is seen at $\delta = 4.72$ ppm, whereas the -H attached to double bond carbon is observed at $\delta = 5.29$ ppm. The presence of the above chemical shift on the HETA spectral confirms the formation of the compound. The ^{13}C NMR spectrum of HETA represented by Fig. 3 shows the peak of terminal –**C**H_3 of fatty amide chains and double bond carbons (–**C**H=**C**H–) at $\delta = 13.99$ ppm and $\delta = 129.56$ ppm, respectively. The peaks within $\delta =$ 22.49–33.70 ppm account for –**C**H_2 on the fatty acid chain except for the nitrogen attached –**C**H_2 that is observed at $\delta = 61.88$ ppm.

T. peruviana polyesteramide (TPPEA)

TPPEA formation is confirmed by the presence of a broad peak at 3438.36 cm^{-1} which indicate terminal –OH group, asymmetric and symmetric CH_2 stretching peaks at 2922.95 and 2851.64 cm^{-1} respectively. The stretching of amide carbonyl and that of ester carbonyl group are respectively observed at 1628.92 and 1731.15 cm^{-1}, also the C–O–C asymmetric and symmetric peaks are at 1237.34 and 1305.92 cm^{-1} respectively whereas, the stretching vibration peak of ester C–O is seen at 1168.76 cm^{-1}. The aromatic ring C–H stretching peaks is observed at 721 cm^{-1}.

From ^{1}H NMR spectrum of TPPEA resin (Fig. 4), the presence of the following protons confirms the structure

Scheme 1 Synthesis of HETA

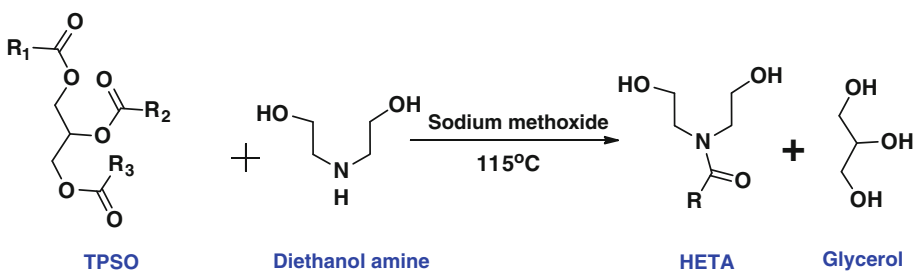

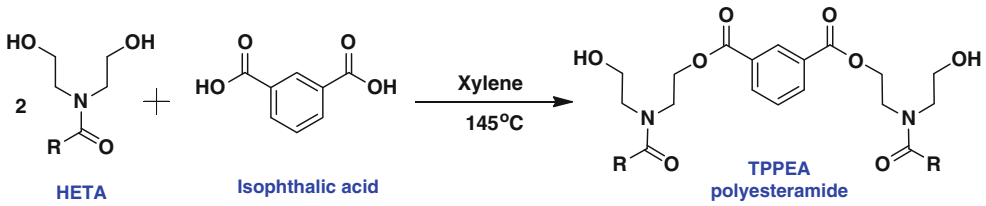

Scheme 2 Synthesis of TPPEA

Scheme 3 Synthesis of APTMS modified ZnO nanoparticles

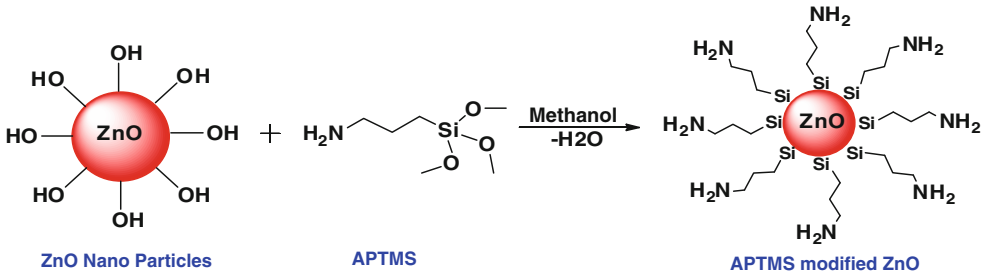

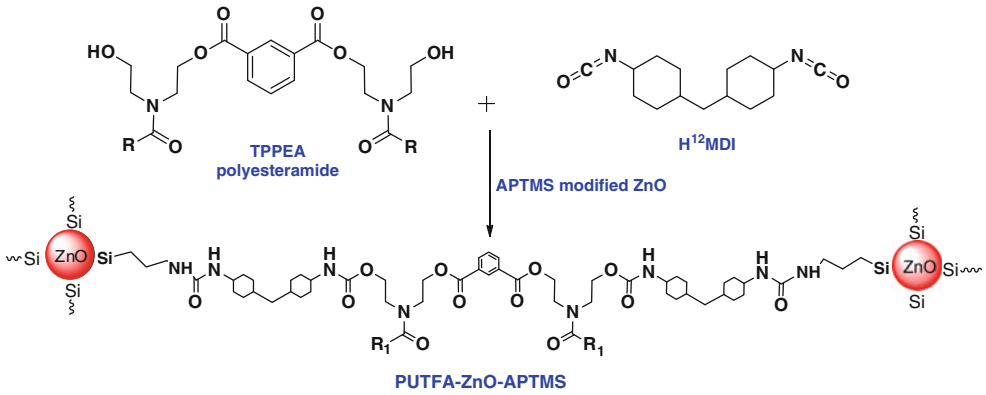

Scheme 4 Schematic representation for synthesis of polyurethane hybrids

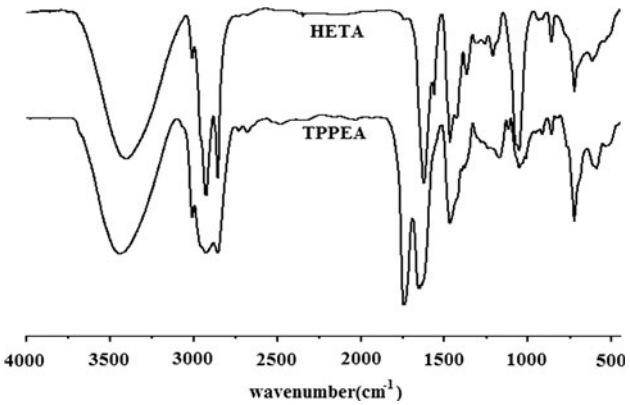

Fig. 1 FTIR spectra of HETA and TPPEA

shown in Scheme 2. The peaks at $\delta = 0.86$–0.89 ppm for terminal methyl group of the fatty acid chains, and $\delta = 1.24$–1.30 ppm peak may be due to the CH_2 group attached to the terminal methyl group as well as that of the internal CH_2 of the fatty acid chains. The hydrogen protons attached to unsaturated carbons appears at $\delta = 5.35$ ppm, the CH_2 adjacent to the ester group is seen at $\delta = 4.52$ ppm while the CH_2 attached to amide nitrogen is observed at $\delta = 3.60$ ppm. The CH_2 group before the terminal alcoholic –OH appears at $\delta = 3.79$ ppm, the ring protons of isophthalic acid is seen at $\delta = 7.55$ ppm, $\delta = 8.21$ ppm and $\delta = 8.64$ ppm.

Poly (urethane fatty amide) resin (PUTFA) and its hybrid films

Figure 5 shows the FTIR of the pristine and that of the hybrid coatings samples, the analysis revealed the similarities in the spectral pattern of PUTFA and its hybrid forms. Differences are only seen in the intensity of their peaks. As observed in Fig. 5, the non appearance of a peak within the –NCO region of the FTIR (i.e. 2100–2270 cm^{-1}) is a clear indication of urethanation reaction between TPPEA and $H_{12}MDI$. The –NH stretching peak for PUTFA and the hybrids are observed between

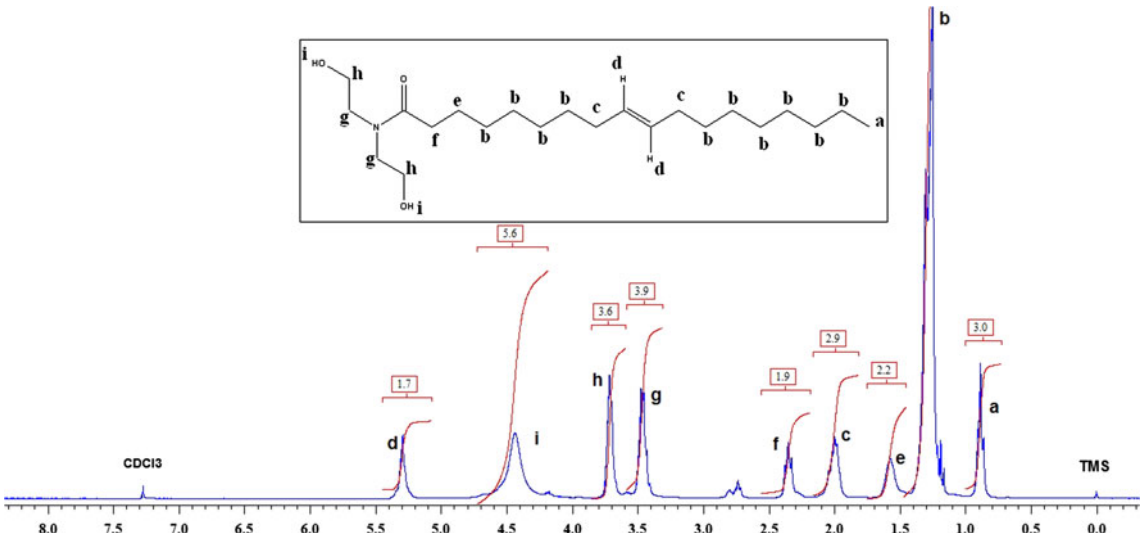

Fig. 2 ^{1}H NMR spectrum of HETA

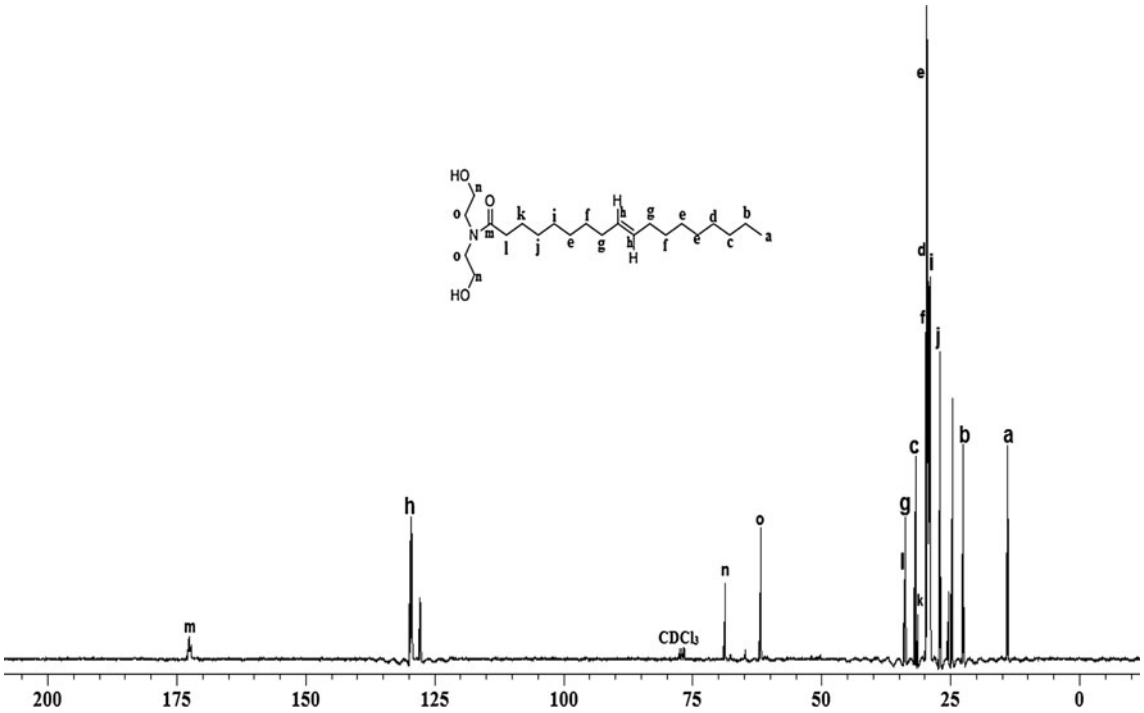

Fig. 3 ^{13}C NMR of HETA

3318.25 and 3327.21 cm^{-1}, it is however observed that the intensity of the peak increases as the percentage APTMS-ZnO in the films increases, this may be due to the frequency in the coupling of the terminal –NCO and the terminal amine on the modified ZnO particle. The 984.25 cm^{-1} corresponds to Si–O–Zn which is an indication of covalent bonding between ZnO and APTMS on the nano particle surface. The stretching asymmetric and symmetric absorption bands for $–CH_2$ of the fatty amide chains appears at 2918.97 and 2850.89 cm^{-1}, while the –CH stretching for the unsaturation is seen at 3004.61 cm^{-1}. The carbonyl amide vibration band is observed within 1632.87–1636.84 cm^{-1} and the C–N stretching peak appears at 1417.11 cm^{-1}. The 1722–1724 cm^{-1} is a significant C=O peak of urethane linkages. More details on FTIR spectroscopy on this study are highlighted on Table 1.

The ^{1}H NMR spectrum of PUTFA as shown in Fig. 6 reveals the peaks of the terminal protons of the fatty amide at $\delta = 0.87$ ppm, the characteristic signal at 8.19 ppm

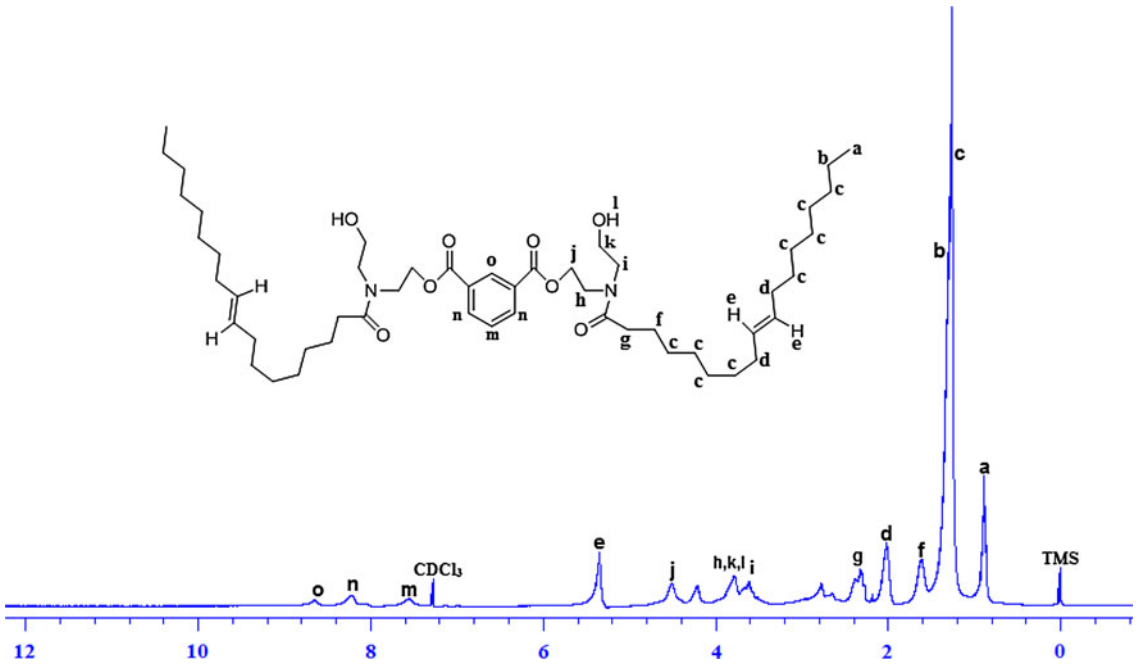

Fig. 4 ^{1}H NMR of TPPEA

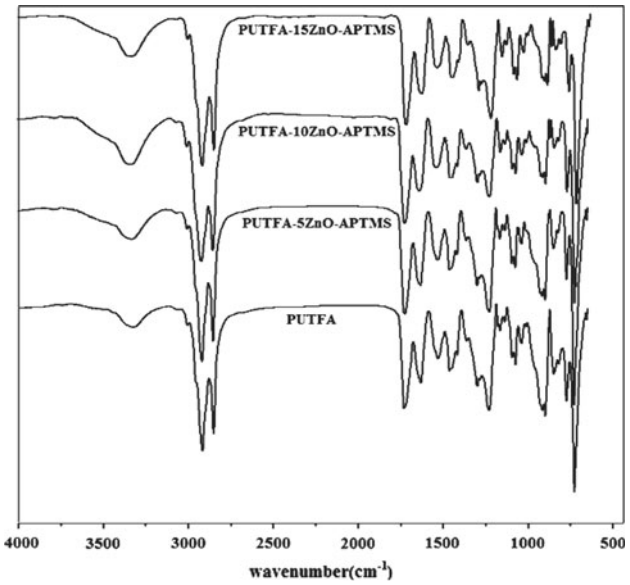

Fig. 5 FTIR spectra of PUTFA and different PUTFA-hybrid coatings

Table 1 FTIR spectra of HETA, TPPEA, PUTFA

Functional group	Wave number (cm^{-1})		
–OH	3370.07	3438.36	–
>C=O (amide)	1622.56	1628.92	1632.87
>C=O (ester)	–	1731.15	1723.87
C–N str. (amide)	1466.70	1442.16	1417.11
CH_2 (asym)	2924.31	2922.95	2918.25
CH_2 (sym)	2853.58	2851.64	2850.59
C=C–H str.	3007.56	3005.49	3004.58
=C–H bend	721.94	727.11	728.61
C–O (ester)	–	1168.76	1165.34
C-O (alc.)	1052.69	1072.74	–
C–O–C (asym)	–	1237.34	–
C–O–C (sym)	–	1305.92	–
>C=O (urethane)	–	–	1723.87
N–H (urethane)	–	–	3318.25
N–H (deformation)	–	–	1530.45
C–N str. (urethane)	–	–	1231.31

assigned to hydrogen (N–H) of the urethane group and the resonance peak at 4.50 ppm ascribed to methylene protons attached to oxygen linking the urethane functional group (–C**H**$_2$–O–CO–NH–) are important confirmations affirming the formation of the urethane. Meanwhile, the chain methylene protons on the fatty amide resonate at 1.30 ppm, α CH_2 attached to the ester is seen at $\delta = 4.51$ ppm.

Physico-chemical characteristics

The physical property of TPSO used as a base material for the preparation of resins under study is compared with other drying and non-drying oils such as Linseed, *Annona squamosa*, *Pongamia glabra*, Soybean and others as contained in Table 2. The TPSO has about 69 % unsaturated

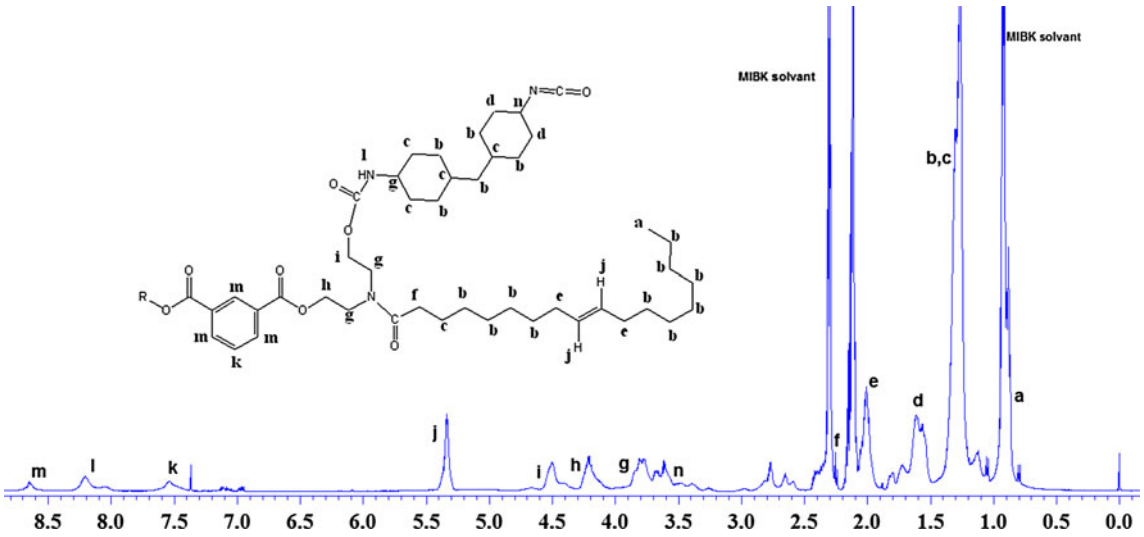

Fig. 6 ^{1}H NMR of PUTFA

fatty acids within the fatty acid profile, oleic acid has the highest percentage of about 48.24 % composition but palmitoleic and erucic acid both have less than 1 % composition. The solubility of the monomer/oligomer as well as the resins were tested in solvents like xylene, DMSO, DMF, methyl isobutyl ketone (MIBK), ethanol, methanol, acetone, chloroform, ether and toluene. HETA shows good solubility in ethanol and methanol apparently due to the terminal –OH on the compound. It also shows about 70–100 % solubility in xylene, chloroform and toluene but insoluble in other above listed solvents. TPPEA resin also showing excellent solubility (90–100 %) in the solvents tested. Figure 7 shows the pictorial representation of transparency retention of the hybrid films. Table 3 highlight some physico-chemical properties of HETA, TPPEA, PUTFA and its hybrid forms. As the percentage weight of the modified nano material doped with the pristine polyesteramide–urethane increases the specific gravity and refractive index of the hybrid systems is also increases. Also, the decrease in the iodine values as well as saponification values form HETA to TPPEA and later PUTFA, PUTFA-APTMS-ZnO (5 wt%) and PUTFA-APTMS-ZnO (10 wt%) reaffirm the cross linking tendencies within the polymer matrix hence, molar mass increase.

SEM analysis

The SEM micrographs of ZnO nano powder, the modified form (APTMS-ZnO) and that of the hybrid films are represented in Fig. 8. The aggregation seen in the inorganic ZnO nano-material is somewhat reduced when compared with that of its modified APTMS-ZnO form, this may be due to steric repulsion on the part of the grafted organic groups attached to the peripheral of ZnO powder. However, the SEM micrographs is showing indication of uniformly distributed nano-particle within the polymer matrix though as the percentage of the nano particle in the polymer matrix increases (i.e. on PUTFA-APTMS-ZnO [15 wt%]) the roughness on the surface thus increase too.

Thermal analysis

The relative thermal stability of PUTFA and PUTFA nanocomposite hybrid films was evaluated from the TGA data derived from the thermogravimetric analysis in N_2 environment. The thermogravimetric and first derivative TG thermogram of all the samples were represented in Figs. 9 and 10 respectively. The characteristic thermal decomposition temperatures such as onset decomposition temperature (T_{ON}), 50 % weight loss temperature, maximum decomposition temperature and %wt remaining at 350, 400, 450 °C for different polyurethane hybrids are reported in Table 4. For instance, the onset decomposition and 50 %wt loss temperatures of PUTFA, PUTFA-ZnO, PUTFA-APTMS-ZnO (5 wt%), PUTFA-APTMS-ZnO (10 wt%), and PUTFA-APTMS-ZnO (15 wt%) are 228.28, 232.26, 233.59, 234.25, 215.68 and 284 °C; 350, 357, 360, 372 and 365 °C respectively. Results show that thermal stability of the polyurethane improved with the percentage addition of ZnO nano material up to 10 wt% loading after that it is reducing may be due to agglomeration of the nano particles. The differential TG thermogram shows that the degradation of the polyurethane hybrid films majorly in two step process. First step degradation corresponds to ester and amide groups and the second step degradation corresponds to urethane and urea groups [45]. The overlay of DSC thermograms of all the polyurethane hybrids is represented in Fig. 11. The glass transition temperatures

Table 2 Characterization of TPSO and its equivalence with other reported triglycerides

Characteristic property	TPSO	Linseed [13]	PGO [13]	SBO [22]	ASO [13]
% of oil content	65	18	33	20	20
Refractive index	1.440	1.478	1.475	1.473	1.475
Iodine value	74.90	161.00	82.00	133.00	88.00
Acid value	2.0	8.3	8.0	0.4	10
Specific gravity	0.912	0.896	0.932	0.925	0.927
Saponification value	194	160	159	190	–
Fatty acid profile					
Oleic acid	48.3	22.0	71.0	22.8	46.0
Palmitic acid	22.1	–	9.2	7.0	–
Linoleic acid	20.2	14.0	14.5	50.8	25.8
Stearic acid	7.3	–	2.0	2.0	–
Arachidic acid	1.4	–	–	< 1.0	–
Palmitoleic	0.3	–	–	< 0.5	–
Margaric acid	0.1	–	–	–	–
Linolenic acid	–	44.0	–	6.8	1.4

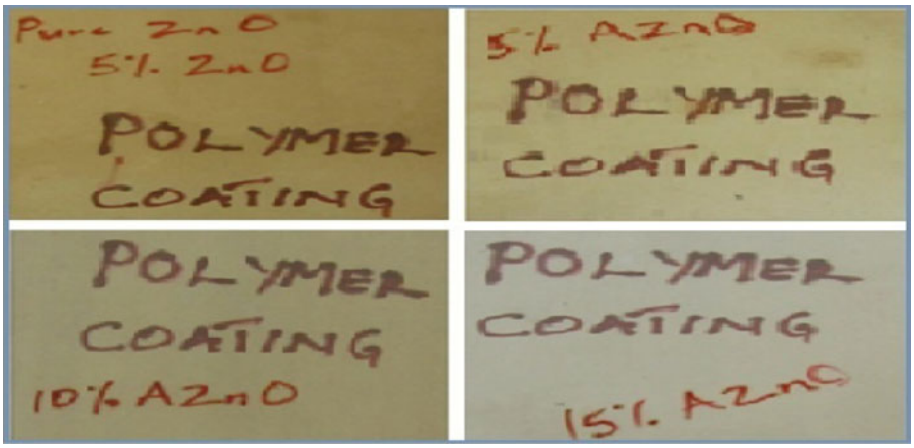

Fig. 7 Photograph showing the retention transparency of hybrid coatings

Table 3 Physico-chemical properties of HETA, TPPEA, PUTFA

Characteristic property	HETA	TPPEA	PUTFA	P-AZ5	P-AZ10
Acid value (mg KOH/g)	3.4	9.7	–	–	–
Iodine value (gICl/100 g)	37.6	21.2	17.3	15.1	13.4
Specific gravity	0.923	0.943	0.947	0.960	0.972
Refractive index	1.467	1.587	1.631	1.642	1.654
Saponification value (mg KOH/g)	195.5	180	165	160	149

P-AZ5 PUTFA-APTM- ZnO (5 wt%), *P-AZ10* PUTFA-APTMS-ZnO (10 wt%)

(T_g) of all the samples noticed in between 140 and 160 °C and also the nanoparticle loaded polyurethane samples are showing slight improvement in the T_g. The increase in thermal stability and glass transition temperature with ZnO nano particles content may be due to the formation of strong network structures through hydrogen bonding by surface hydroxyl groups of ZnO and urethane groups. These type of crosslinked structures act as a thermal insulator and mass transport barrier to the volatile products generated during decomposition and thus increases the degradation temperature [36].

Antibacterial study

The antibacterial testing of PUTFA, PUTFA-ZnO (5 wt%) and other hybrid forms was carried out in *E. coli, S. aureus, K. pneumoniae* and *B. subtilis* as test organisms because they are common pathogenic organisms [46, 47]. The antibacterial results of the coating films are summarized in Table 5, though antibacterial activity was actively mild for PUTFA on *E. coli* and *S. aureus* it was inactive for

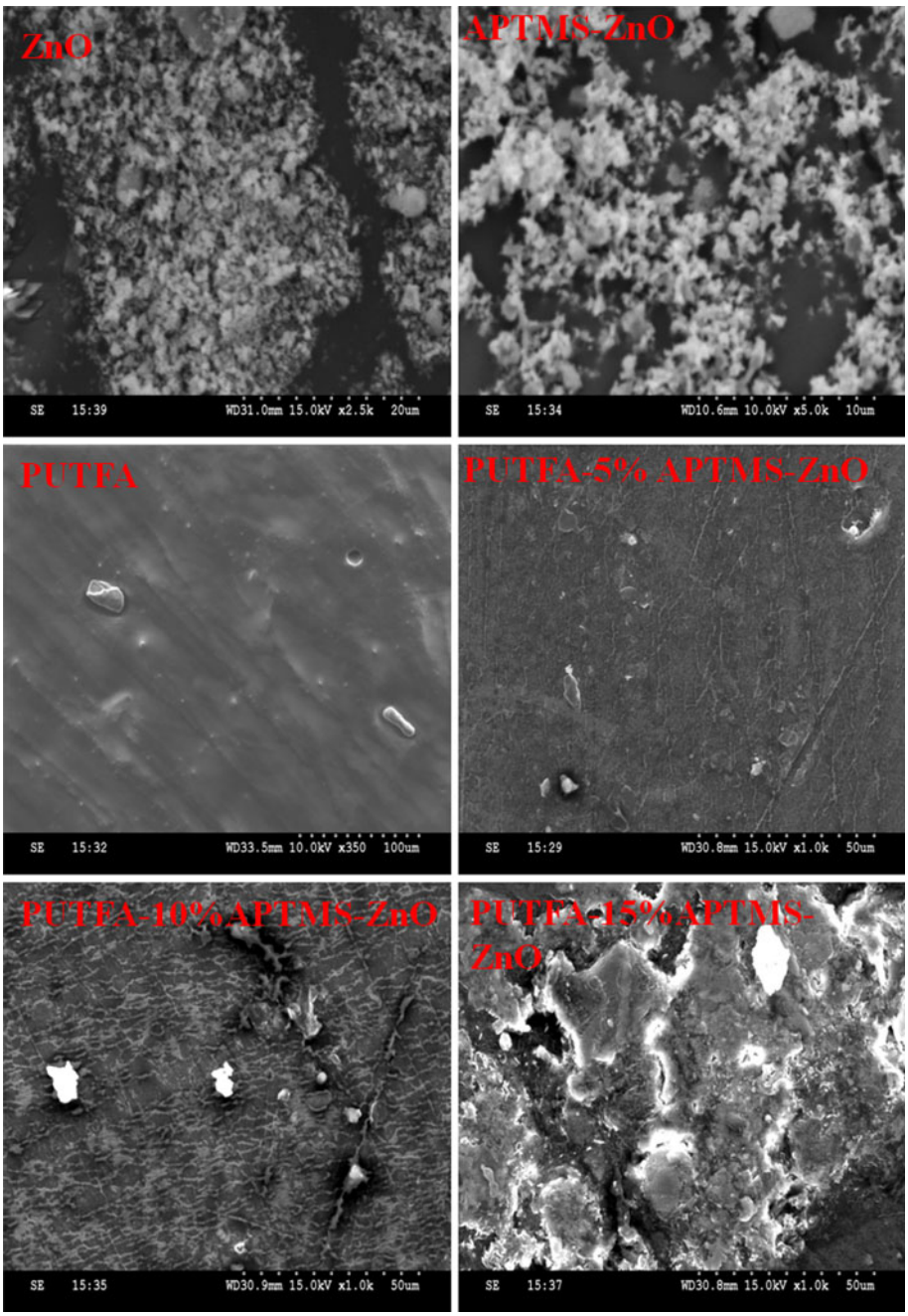

Fig. 8 SEM micrographs of ZnO, APTMS-ZnO, PUTFA and PUTFA-hybrids

K. pneumoniae and *B. subtilis*. PUTFA-APTMS-ZnO (5 wt%) and PUTFA-APTMS-ZnO (10 wt%) both exhibited the highest antibacterial activity on *E. coli*, it is however noticed that PUTFA-APTMS-ZnO (15 wt%) shows antibacterial activity less than that of PUTFA-APTMS-ZnO (5 wt%) and PUTFA-APTMS-ZnO (10 wt%) in *E. coli* even though it has higher percentage content of nano-material. This observation may be due to inadequate spread of the nano-material within the polymer matrix thereby showing a moderate activity in *E. coli* and *S. aureus*. The coating films examined it this study shows inactive antibacterial status in *B. subtilis*. The antibacterial activity shown by the hybrid films can be attributed to the presence of zinc oxide nano particles [34].

Drying behaviour and fog test results

The anticorrosive properties as well as drying time of PUTFA and it hybrid resins are summarized in Table 6. The influence of doping the polymeric matrix of PUTFA with ZnO-APTMS in varying percentages on the anticorrosive properties and drying time was investigated. A notable difference was observed on mild steel coated with hybrid resins, the hybrid resin gives faster drying time when compared with

that of PUTFA, and this attribute improves as the percentage of nano-material within the polymer matrix increases. The fast drying property exhibited by the hybrid resin on mild strips can be ascribed to siloxane coupling network which has made the resin to be denser. The corrosion resistance of the coating was evaluated by salt spray test results. The salt spray test results of PUTFA and different hybrid coatings (PUTFA-APTMS-ZnO) over mild steel panels are shown in Fig. 12a, b. This shows the result of the salt spray test of PUTFA/APTMS-ZnO hybrid coatings before and after 308 h of salt mist test in 3.5 % NaCl solution. Fig. 11b reveals the conditions of the coated panels that were cross cut diagonally. In all, panels with hybrid coating show better coating resistance; this improves as the nano-material load increases. PUTFA-APTMS-ZnO (5 wt%), PUTFA-APTMS-ZnO (10 wt%) and PUTFA-APTMS-ZnO (15 wt%) possess better corrosion resistance when compared with PUTFA and PUTFA-5ZnO.

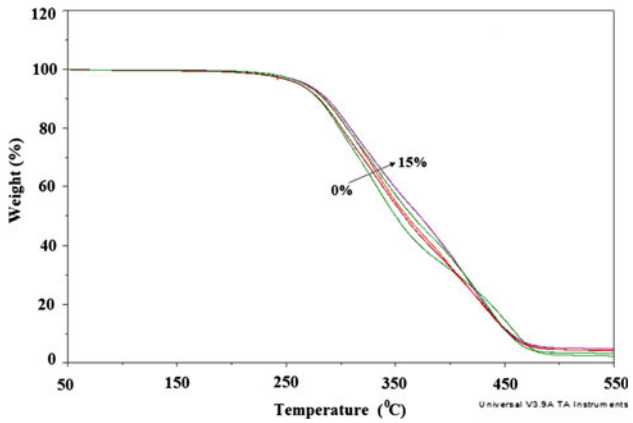

Fig. 9 TGA curves of PUTFA and nanocomposites

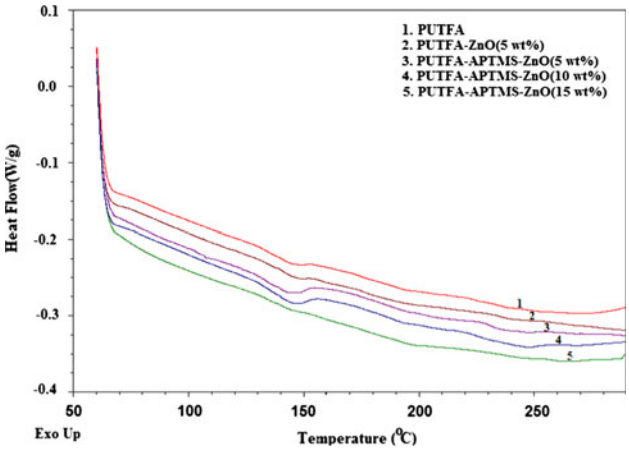

Fig. 11 DSC thermograms of PUTFA and PUTFA-hybrids

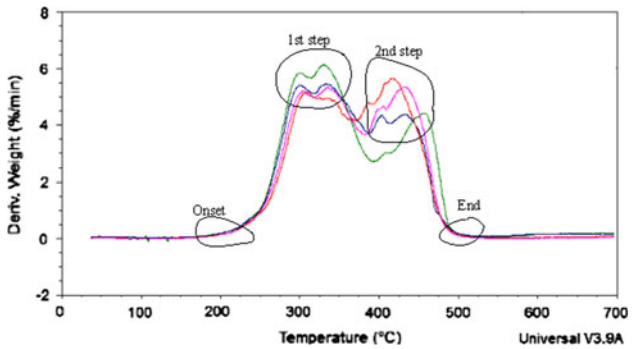

Fig. 10 Derivative of TGA curves

Table 5 Antibacterial activities of PUTFA and its hybrids

Resin code	P	P-5ZnO	P-APTMS-ZnO (5 wt%)	P-APTMS-ZnO (10 wt%)	P-APTMS-ZnO (15wt %)
E. coli	+	++	+++	+++	++
S. aureus	+	++	++	++	++
K. pneumoniae	–	–	+	+	+
B. subtilis	–	–	–	–	–

P PUTFA, – inactive, + mildly active, ++ moderately active, +++ highly active

Table 4 Thermal behaviour of PUTFA and its hybrids

Sample codes	T_{ON} (°C)	T_d 50 % (°C)	T_{1Max} (°C)	Wt% remaining at 350 °C	Wt% remaining at 400 °C	Wt% remaining at 450 °C	Tg (°C)
PUTFA	228.28	350	269.72	49.84	31.92	14.43	138.79
PUTFA-ZnO	232.26	357	271.21	53.71	32.64	11.49	148.97
PUTFA-APTMS-ZnO(5 wt%)	233.59	367	273.56	54.78	33.15	11.15	149.84
PUTFA-APTMS-ZnO(10 wt%)	234.25	372	277.52	59.34	37.07	11.72	150.01
PUTFA-APTMS-ZnO(15 wt%)	215.68	365	271.23	56.96	35.92	11.25	150.43

T_{ON} onset decomposition temperature, $T_d 50$ % 50 % wt loss temperature, $T_{1\ Max}$ maximum decomposition temperature

Table 6 Chemical resistance and drying time of PUTFA and its hybrid forms

Resin code	P	P-5ZnO	P-APTMS ZnO (5 wt%)	P-APTMS ZnO (10 wt%)	P-APTMS ZnO (15 wt%)
Drying time[a] (day)	5	3	2	1	1
H_2O (10 days)	A	A	A	A	A
NaOH (5 %, 2 h)	C	B	A	A	B
HCl (5 % 10 days)	B	B	A	A	B

P PUTFA, *A* unaffected, *B* slightly loss of gloss, *C* film partially removed

[a] Ambient cured

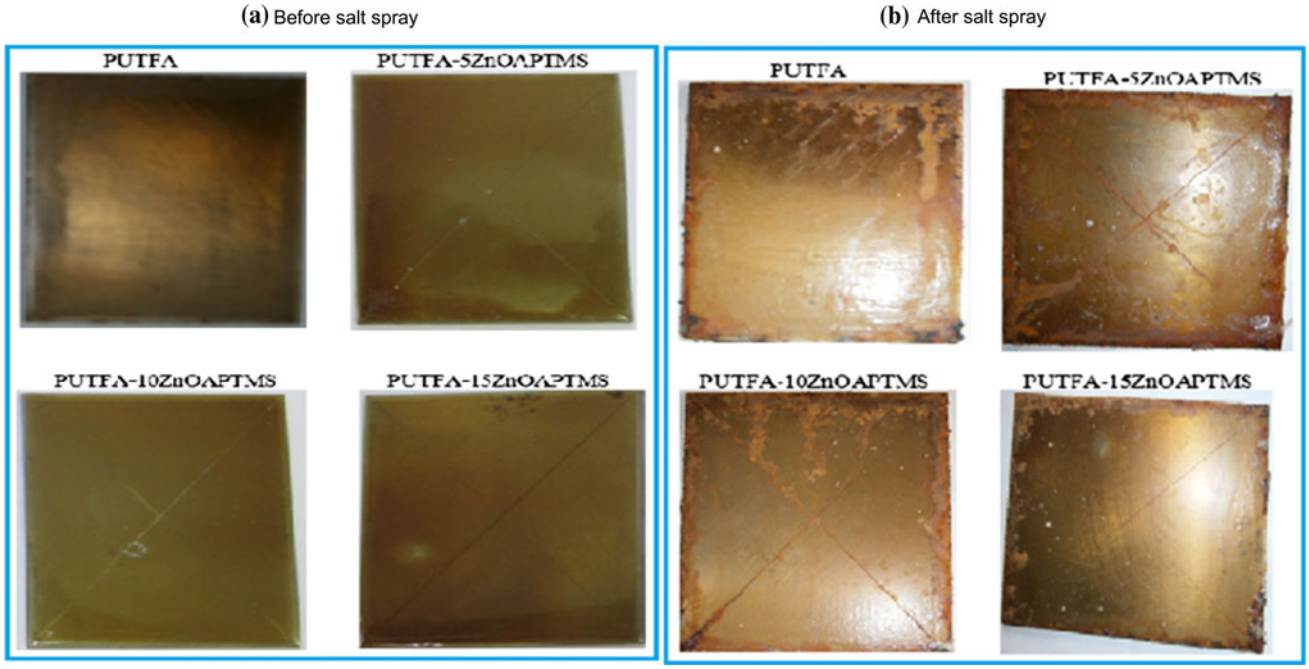

Fig. 12 The salt spray results of pristine and hybrid coatings in 3.5 % NaCl solution

Conclusions

The incorporation of APTMS modified ZnO within the polymer matrix of PUTFA was successful. This air drying nano-composite prepared from TPSO-based polyesteramide–urethane showed improved antibacterial properties except for *B. subtilis*. The thermal stability of the coatings was enhanced as APTMS-ZnO percentage increases within the PUTFA matrix. The coatings retain their photographic transparency irrespective of the varying inorganic–organic nano-particle within the polymer matrix. The studies signal the inherent potential of this modified hybrid coating as an eco-friendly anticorrosive and anti microbial coatings from TPSO.

Acknowledgements The author Tolutope O. Siyanbola is grateful to TWAS and CSIR (India) for the TWAS-CSIR Postgraduate Fellowship Award. Siyanbola is also thankful to Prof. K.O. Okonjo, Oladele O. James and Mrs Tunmike S. Siyanbola for their evergreen encouragements.

References

1. Meier MAR, Metzger JO, Schubert US (2007) Chem Soc Rev 36:1788
2. Özgür Seydibeyoğlu M, Misra M, Mohanty A, Blaker JJ, Bismarck A, Kazemizadeh M (2013) J Mater Sci 48. doi 10.1007/s10853-012-6992-z
3. Baumann H, Buhler M, Fochem H, Hirsinger F, Zoebelein H, Falbe J (2003) Angew Chem. In. Ed 27:41
4. Siyanbola TO, Ajanaku KO, James OO, Olugbuyiro JAO, Adekoya JO (2011) J Pure and Appl Sci 1:49
5. Padma LN et al (2000) Polym Rev 40:1
6. MacGregor EA, Greenwood CT (1980) Polymers in nature. Wiley, New York
7. Larock RC, Lu Y (2009) ChemSusChem 2:136
8. Aigbodion AI, Pillai CKS, Bakare IO, Yahaya LE (2001) Indian J Chem Technol 8:378
9. Ahmad S, Ashraf SM, Naqvi F, Yadav S, Hasnat A (2001) J Polym Mater 18:53
10. Alam M, Sharmin E, Ashraf SM, Ahmad S (2004) Prog Org Coat 50:224
11. Zafar F, Ashraf SM, Ahmad S (2004) Prog Org Coat 51:250
12. Trevino AS, Trumbo DL (2002) Prog Org Coat 44:49

13. Yadav S, Zafar F, Hasnat A, Ahmad S (2009) Prog Org Coat 64:27
14. Ahmad S, Ashraf SM, Naqvi F, Yadav S, Hasnat A (2003) Prog Org Coat 47:95
15. Dutta N, Karak N, Dolui SK (2004) Prog Org Coat 49:152
16. Kanai T, Mahato TK, Kumar D (2007) Prog Org Coat 58:259
17. Samadzadeh M, Boura SH, Peikari M, Ashrafi A, Kasiriha M (2011) Prog Org Coat 70:383
18. Ahmad S, Naqvi F, Sharmin E, Verma KL (2006) Prog Org Coat 55:268
19. Li F, Larock RC (2000) J Appl Polym Sci 78:1044
20. Deka H, Karak N (2009) Prog Org Coat 66:192
21. Nandan V, Joseph R, George KE (1999) J Appl Polym Sci 72:487
22. Motawie AM, Hassan EA, Manieh AA, Aboul-Fetouh ME, El-Din F (1995) J Appl Polym Sci 55:1725
23. Güner FS, Yağci Y, Erciyes AT (2006) Prog Polym Sci 31:633
24. Akintayo CO, Akintayo ET, Ziegler T (2011) Prog Org Coat 71:89
25. Zafar F, Ashraf SM, Ahmad S (2007) J Appl Polym Sci 104:51
26. Nylen P, Sunderland E (1965) Modern surface coatings. Wiley, London, p 213
27. Ahmad S, Ashraf SM, Hasnat A, Yadav S, Jamal A (2001) J Appl Polym Sci 82:1855
28. Ahmad S, Ashraf SM, Sharmin E, Zafar F, Hasnat A (2002) Prog Cryst Growth 45:83
29. Jayakumar R, Rajkumar M, Nagendran R, Nanjundan S (2002) J Appl Polym Sci 85:1194
30. Ahmad S, Zafar F, Sharmin E, Garg N, Kashif M (2012) Prog Org Coat 73:112
31. Jayakumar R, Nanjundan S, Rajkumar M, Nagendran R (2001) J Macromol Sci Pure Appl Chem A 38:869
32. Uhlig HH, Revie RW (1985) Corrosion and corrosion control: an introduction to corrosion science and engineering, 3rd edn. Wiley, New York
33. Badri KH, Shahaldin FH, Othman Z (2004) J Mater Sci 39. doi:10.1023/B:JMSC.0000033419.16121.a0
34. Jayakumar R, Lee Y-S, Nanjundan S (2003) React Funct Polymer 55:267
35. Jayakumar R, Radhakrishnan S, Nanjundan S (2003) React Funct Polymer 57:23
36. Mishra AK, Mishra RS, Narayan R, Raju KVSN (2010) Prog Org Coat 67:405
37. Jena KK, Rout TK, Narayan R, Raju KVSN (2012) Polym Int 61:1101
38. Ibiyemi SA, Fadipe VO, Akinremi OO, Bako SS (2002) J Appl Sci Environ Manag 6:61
39. Obasi NB, Igboechi AC (1991) Fitoterapia 62:159
40. Zibbu G, Batra A (2011) J Pharm Res 4:4461
41. Dutta AC (1964) Botany for degree students, 5th edn. Oxford University Press, London, p 742
42. Linday ME (1962) Practical introduction to microbiology. E and F.N. Spon Ltd., London, p 177
43. Adewuyi A, Oderinde RA, Rao BVSK, Prasad RBN (2011) J Surfact Deterg 15:89
44. Misiev TA (1991) Powder coatings chemistry and technology. Wiley, New York, p 203
45. Janvi I, Petrovic ZS, Guo A, Fuller R (2000) J Appl Polym Sci 77:1723
46. Kenawy E, Abdel Hay FI, El-Raheem A, El-Shanshoury R, El-Newehy MH (2000) J Polym Chem 40:2384
47. Hazziza-Laskar J, Helary G, Sauvet G (1995) J Appl Polym Sci 58:77